INSTITUTE FOR NUCLEAR STUDY
UNIVERSITY OF TOKYO
Tanashi-Shi, Midori-Cho
Tokyo, Japan

INS-TH- 118
November 1978

Beam Loading Effects in a Standing Wave Accelerator Structure

Shigeaki ARAI, Takeshi KATAYAMA,

Eiki TOJYO and Katsuhide YOSHIDA

INS-TH- 118
November 1978

Beam Loading Effects in a Standing Wave Accelerator Structure

Shigeaki ARAI, Takeshi KATAYAMA, Eiki TOJYO and Katsuhide YOSHIDA
Institute for Nuclear Study, University of Tokyo
Tanashi-shi, Tokyo 188

Abstract

The steady-state beam loading effects on the accelerating field in the disk-loaded structure of a standing wave type have been systematically studied. The electron bunch from a 15 MeV electron linac is injected at arbitrary phase of the external driving field in the test structure. The change of the phase shift of the accelerating field and that of the stored energy are measured as a function of the phase on which the bunch rides. The former shows drastic change when the bunch is around the crest of the driving field and when the beam loading is heavy, whereas the latter varies sinusoidally for any beam loading. The resonant frequency shift of the structure due to beam loading is estimated by using the measured results. All the experimental results are well explained by the normal mode analysis of the microwave cavity theory.

§1 Introduction

With the development of accelerator utilization, it is contemporary requirement for the accelerator technology to increase the intensity, to suppress the energy spread and to improve the stability of the output beam. In achieving these objects, one can not neglect the beam loading effect on the accelerating field. This effect is especially serious in linear accelerator (linac) because it usually accelerate very intense beam.

The effect of steady-state beam loading can be regarded as to be caused by the electromagnetic field induced in the accelerator structure by the bunched beam. Among the Fourier components of the induced field, the fundamental mode give rise to so-called detuning of the accelerator structure, which will affect the intensity and the energy spectrum of the beam. Instabilities such as beam break-up in large-scale electron linac are known to be originated by the induced field of some higher modes. Here we will treat with the problems related to the detuning effect both from experimental and from theoretical aspects.

The detuning of the accelerator structure due to the beam loading has the effect not only on the beam quality but also on the microwave source. The effect on the beam is such that the amplitude reduction and the phase shift of the accelerating field cause the deterioration of the accelerating efficiency and of the energy spectrum. On the other hand, the reflections of the microwave power from the accelerator structure increases because

of the impedance change of the structure, and makes it difficult to operate the microwave source stably.

Methods and devices to compensate for these effects have been studied by many authors[1-4]. Through these studies, the general theory for beam loading phenomena[5-8], based upon the equivalent circuit analysis or upon the microwave cavity theory, has been developed. While the experimental studies of the beam loading[9-11] are so far limited to those around the synchronous phase of the accelerating field or to measurements on simulated systems.

In the present experiment, the bunched beam from the electron linac is passed through the S-band disk-loaded accelerator structure of standing wave type, and the phase of the bunch with respect to the driving field in the structure is systematically varied. To separate the effect on the microwave source, the accelerator structure has been connected to it by well-padded transmission line. Thus the measurements can be the direct test of the beam loading theory.

The following subjects will be discussed in the subsequent sections.

1) Changes of the amplitude and the phase shift of the accelerating field as a function of the initial phase, on which the bunch rides.

2) Relation between the phase shift of the accelerating field and the resonant-frequency shift of the accelerator structure.

3) Application of the normal mode analysis to the experi-

mental results.

§2 Experimental Arrangements

The schematic diagram of the experimental setup and the microwave apparatus is shown in Fig. 1. The test cavity is a disk-loaded waveguide of the standing wave type, which consists of 6 disks, 5 cylinders, 2 half-cylinders and 2 end-plates as seen in Fig. 1. The dimensions of the structure are as follows: the disk-hole diameter 2a is 22.255 mm, the cylinder diameter 2b is 85.056 mm, the periodic length d is 36.233 mm, the disk thickness t is 5.000 mm and the total length of the structure is 21.74 cm. The normalized phase velocity v_p/c and the normalized group velocity v_g/c of the structure are 1.00 and 1.13×10^{-2}, respectively. Each end-plate has a hole of 5 mm in diameter at the center for passing the beam and a small antenna at the distance of 16 mm from the center for microwave coupling, the coupling coefficient of which is 0.05. This structure is assembled on a V-block and is put in the vacuum chamber as shown in Fig. 2.

The microwave power for exciting the structure is supplied from the traveling wave tube amplifier operating pulsively in the microwave system of the linac. The peak power and the pulse width of the microwave to the structure are 16 Watt and 5 μsec, respectively.

The electron beam of the INS (Institute for Nuclear Study, University of Tolyo) linac which has the energy of 15 MeV and

the beam pulse width of 2 μsec, is used as the bunched beam in the present experiment. The output beam from the linac is collimated to have a diameter of 2 mm and is transported to the test structure. The beam current is measured by a Faraday-cup located downstream of the structure.

Since the test structure has the same dimensions as the regular section of the INS linac[12], its resonant frequency is equal to the operation frequency of the linac if both structures have the same temperature with each other. Then, the linac is operated with the same frequency as the resonant frequency of the structure by temperature controll in order to synchronize the RF field in the structure with the incident electron bunch.

§3 Measurement Method and Experimental Results

The changes of the stored energy and of the phase shift of the microwave field in the structure due to beam loading are measured as a function of the phase of the external driving field for the beam bunch.

In the first place, the stored energy W in the structure can be obtained by measuring the radiated power from the structure, P_{rad}, and by using the relation

$$P_{rad} = \frac{\beta \omega W}{Q_o} \quad , \tag{3.1}$$

where Q_o is the unloaded Q of the structure, ω is the angular frequency of the microwave and β is the coupling coefficient of

the antenna, which can in turn be determined from the relation between the input power P_o and the transmitted power P_t of the structure

$$\frac{P_t}{P_o} = \frac{4\beta^2}{1 + 2\beta} \quad . \tag{3.2}$$

The stored energy purely due to the beam-induced field, W_b, can be measured by the experimental arrangement of Fig. 1, but without feeding the external microwave. An example of the waveform of the induced field is shown in Fig. 3. It is seen in the figure that the field is built up in the beam pulse duration (2μ second) and then decays gradually. The peak of the waveform corresponds to P_{rad} at the pulse end and for a certain peak beam intensity which can be found from the average current measured by the Faraday cup and from the duty factor of the beam. Fig. 4 shows the peak stored energy as a function of the beam current thus measured. The solid line in the figure is the calculation with the same parameters as the experiment (see Appendix A). Fairly good agreement of both results confirms the validity of the present experimental procedure.

The waveforms of energy storing in the structure excited by the external microwave are shown in Figs. 5(a) ∿ 5(c). Fig. 5(a) represents the P_{rad} without the electron beam. Fig. 5(b) shows the build up of the field when the electron bunches are injected into the structure at the accelerating phase and are taking the energy off the driving field. Fig. 5(c) corresponds to the case when the bunches are at the decelerating phase and are giving the

energy to the structure.

The phase of the driving field for the electron bunch can be adjusted by use of the line stretcher located between the structure and the external microwave source, as seen in Fig. 1. One can know the scale of the line stretcher with which the electron bunch is ridden just on the crest of the accelerating or of the decelerating phase by making the stored energy minimum or maximum, and hence can realize any phase of the driving field for the electron bunch.

The phase shift of the field in the structure (superposition of the driving field and the induced field) from the original driving field is measured by the following way: The driving microwave power divided from the source is further divided by another directional coupler. One of the branches is used for exciting the structure, and the other is connected to a magic-T for comparing the phase with that of the microwave from the structure (see Fig. 1). At the start of the measurement, the electron beam is turned off and the phase shifter between the structure and the magic-T is adjusted so that the vector summation of the signals to the magic-T is minimized. By this adjustment, the phase difference between two signals at the magic-T is confirmed to be 180 degree. Then, passing the electron beam, the phase shifter is adjusted again to minimize the vector summation. The difference of the scale of the phase shifter between the first and the second measurement provides the phase shift due to the beam loading for given phase of the bunch and intensity of the beam.

Following the method mentioned above, the stored energy and the phase shift of the field in the structure has been measured systematically by varying the phase of the driving field for the bunch and the degree of the beam loading. We have defined the beam loading in terms of the ratio of the beam induced field E_b to the external driving field E_o, which is given by

$$\frac{E_b}{E_o} = \sqrt{\frac{W_b}{W_o}} \quad . \tag{3.3}$$

Here W_b and W_o are the stored energies due to induced field and due to driving field, respectively, as discussed before.

The measurement has been performed for E_b/E_o of 0.30 and 0.62. The results are shown in Fig. 6 by open circles for the stored energy and by solid circles for the phase shift, as a function of the relative phase of the electron bunch to the driving field. The absolute value of the phase of the bunch for the driving field is so defined that it is zero and 180 degree when the bunch is on the crest of the accelerating and of the decelerating phase, respectively. The upside diagram in the figure represents the slight beam loading case, $E_b/E_o = 0.30$ and the downside one is for the heavy beam loading case, $E_b/E_o = 0.62$.

The remarkable features of the results are as follows:

1) The stored energy changes like sinusoidally for the phase of the electron bunch.

2) The phase shift is negligible for the resistive beam loading, that is for the phases of the bunch of zero or 180

degree, at least for the beam loading factor E_b/E_o under 0.62.

3) The phase of the field changes drastically for the reactive beam loading, that is for the phases of the bunch exept zero and 180 degree. The phase shift varies steeply near zero degree, especially when the beam loading is heavy.

§4 Theoretical Analysis and Discussion

The experimental results presented in the preceeding section are analyzed by the normal mode analysis of the microwave cavity theory[6,7,13,14]. In the analysis, the other modes than the fundamental mode are neglected. This is justified by the spectrum measurement on the induced field, in which the fundamental mode has turned out to be intensive by 30 db compared to any other mode (See Appendix B).

Now we will treat with the phenomena expected in the accelerator structure into which the external microwave is fed and also the electron bunches are injected.

In the first place, the stored energy can be expressed as

$$W = \frac{4P_o}{\omega Q_{ext\cdot 1}} \frac{1}{\left(\frac{1}{Q_{ext\cdot 1}} + \frac{1}{Q_{ext\cdot 2}} + \frac{1}{Q_o} + \frac{1}{Q_b}\right) + \left(\frac{2\Delta\omega}{\omega_a'}\right)^2}, \quad (4.1)$$

where P_o is the input microwave to the structure, $Q_{ext\cdot 1}$, $Q_{ext\cdot 2}$ are the external Q for the input and the output coupler, respectively, Q_b is the beam Q, ω_a' is the resonant frequency of the structure without beam and $\Delta\omega$ is the resonant frequency shift

due to reactive beam loading (See Appendix C). Q_b and $\Delta\omega = \omega - \omega_a'$ are given by the following equations[6)]

$$\frac{1}{Q_b} = \frac{1}{Q_L} \frac{B\cos\phi_b - B^2}{1 + B^2 - 2B\cos\phi_b} \quad , \tag{4.2}$$

$$\frac{2\Delta\omega}{\omega_a'} = \frac{1}{Q_L} \frac{-B\sin\phi_b}{1 + B^2 - 2B\cos\phi_b} \quad , \tag{4.3}$$

Where Q_L is loaded Q, B is the ratio of the beam induced field E_b to the driving field E_o, E_b/E_o, and ϕ_b is the relative phase of the bunch to the driving field as defined in the preceeding section and shown in Fig. 7.

Substituting eqs. (4.2) and (4.3) into eq. (4.1), we obtain an expression for the stored energy W as a linear function of $\cos\phi_b$

$$W = \frac{4P_o Q_L^{\,2}}{\omega Q_{ext\cdot 1}} (1 + B^2 - 2B\cos\phi_b) \quad , \tag{4.4}$$

where $4P_oQ_L^{\,2}/\omega Q_{ext\cdot 1}$ is the stored energy without the beam loading.

This equation explains well the experimental result that the stored energy changes sinusoidally for the variation of ϕ_b. The curves in Fig. 6 are the numerical results of eq. (4.4) for B = 0.30 and 0.62.

The field in the structure is the superposition of the driving field and the beam-induced field;

$$Ee^{j(\omega t + \psi)} = E_o e^{j\omega t} - E_b e^{j(\omega t + \phi_b)} \quad , \tag{4.5}$$

where ψ is the phase shift between the resultant field and the driving field and can be expressed as

$$\psi = \tan^{-1}\left(\frac{-B\sin\phi_b}{1 - B\cos\phi_b}\right) \quad , \tag{4.6}$$

The calculated results for B = 0.30 and 0.62 are shown in Fig. 6.

We are interested in the resonant frequency shift due to beam loading. The pulse length of the driving microwave and of the electron beam, however, are not sufficiently long for us to measure the frequency shift directly. Then it is estimated from the measured quantities.

In the first place, one can calculate the resonant frequency shift from the beam loading factor B by using eq. (4.3). The result is shown in Fig. 6 by solid line. On the other hand, it is possible to get the frequency shift from the measured phase shift. Combining eqs. (4.2), (4.3) and (4.6), one obtains the relation

$$\psi = \tan^{-1}\left(\frac{2\Delta\omega}{\omega_a} Q_T\right) \quad , \tag{4.7}$$

where $\frac{1}{Q_T} = \frac{1}{Q_L} + \frac{1}{Q_b}$.

This is familiar equation for estimating the phase shift conversely when the operating frequency is different from the resonant frequency of the cavity. Since the beam Q, Q_b in the eq. (4.7) can not be measured, it is calculated by using eq. (4.2). Total Q, Q_T thus obtained is shown in Fig. 8.

The resonant frequency shift given by above method is shown in Fig. 6 by cross marks. It is seen that the results estimated by different ways agree with each other.

From the experimental results and the theoretical analysis so far discussed, we can conclude as follows;

1) The resonant frequency shifts to higher frequency when the electron bunch is in the phase where the field is decreasing with time and vice versa. This agrees with the well known fact that the RF acceleration system of the electron synchrotron in which the stable phase is behind the crest of the field is operated with higher frequency than the resonant frequency without the beam, and that the resonant frequency of Alvares proton linac which accelerate low velocity protons and whose stable phase is before the field crest, shifts to lower frequency.

2) The variation of the degree of the phase shift or the resonant frequency shift is most steep around the crest of the field, especially in case of heavy beam loading. This means that the acceleration of the particle which is riding just on the field crest will suffer from the instability of the tuning frequency.

3) The detuning of the structure due to the resistive beam loading has not been observed so far as the beam loading is limited below $B = 0.62$.

4) All the experimental results can be explained by the normal mode analysis including only the fundamental mode. As is evident from the deduction procedure, the results are valid for the steady-state beam loading in any cavity of standing wave type.

Acknowledgements

The authors would like to express their sincere thanks to professor J. Tanaka and Professor K. Huke for helpful discussions on this experiment. They are also grateful to Mr. H. Tsujikawa, Mr. K. Kobayashi and Mr. T. Morimoto for their kind cooperative works at experimental measurements. They are indebted to the members of INS mechanical shop for their skillful construction of the experimental apparatus. The numerical analysis has been carried out with the computer TOSBAC-3400 of the Electronic Computer Section at INS.

Appendix A : Beam-Induced Field

According to J. C. Slater's theory for the hollow cavity, the equation of forced oscillation due to the bunched beam is expressed by

$$\frac{d^2}{dt^2}\int EE_a dv + \frac{\omega_a'}{Q_L}\frac{d}{dt}\int EE_a dv + \omega_a'^2 \int EE_a dv = -\frac{1}{\varepsilon_o}\frac{d}{dt}\int JE_a dv \quad , \qquad (A.1)$$

where E is the electric field, E_a is the a-th normal mode field, J is the current density of the bunched beam and ω_a' is the resonant angular frequency of the cavity without the beam. The beam-cavity coupling integral of the right hand side is given approximately[6] by

$$\int JE_a dv = 2I_o E_{ao} L e^{j\omega_a' t} \quad , \qquad (A.2)$$

if the bunch is composed of the rectangular pulse whose width is relatively short compared to the period of pulses and the bunch is synchronous with the a-th mode. I_o is the beam current averaged over the bunches, E_{ao} is the amplitude of the a-th normal mode field and L is the cavity length.

If the beam is expressed by a step function ($I_o = 0$ when $t \leqq 0$ and I_o = const when $t > 0$) the solution of eq. (B.1) is given by

$$\int EE_a dv = \frac{2Q_L I_o E_{ao} L}{\varepsilon_o \omega_a'} [1 - e^{-(\omega_a'/2Q_L)t}] e^{j\omega_a' t} \quad , \qquad (A.3)$$

The stored energy is defined by

$$W = \frac{1}{2} \varepsilon_o |\int EE_a dv|^2 \quad . \qquad (A.4)$$

Substituting eq. (A.3) into eq. (A.4) we have

$$W = \frac{2Q_L^2 I_o^2 E_{ao}^2 L^2}{\varepsilon_o \omega_a'^2} [1 - e^{-(\omega_a'/2Q_L)t}]^2 \quad . \qquad (A.5)$$

On the other hand, the relation between E_{ao} and the effective shunt impedence, r_s, is given by

$$E_{ao}^2 = \frac{\varepsilon_o \omega_a' r_s}{2Q_o L} \quad . \qquad (A.6)$$

From eqs. (A.5) and (A.6), the energy of the beam-induced field stored in the structure is expressed by the following form;

$$W = \frac{Q_L^2 I_o^2 L r_s}{\varepsilon_o \omega_a'} [1 - e^{-(\omega_a'/2Q_L)t}]^2 \quad . \qquad (A.7)$$

This equation represents the build-up of the beam-induced field which is seen in Fig. 3. For the present experiment, the values of the parameters in eq. (A.7) are as follows:
$Q_L = 10400$, $Q_o = 11400$, $L = 21.74$ cm, $\omega_a' = 1.733 \times 10^{10}$, $r_s/Q_o = 24$ Ω/cm and $t = 2.2$ μsec.

Then the peak stored energy W (joule) can be expressed as the function of current I_o (ampere) ;

$$W = 2.29\ I_o^2 \quad .$$

This relation between I_o and W is shown in Fig. 4 with the solid line.

As seen in the figure, there is slight difference between the calculation and the experiment. This will be due to the approximations that the beam pulse looking like a trapezium with the half width of about 2.2 μsec is regarded to be a 2.2 μsec rectangular pulse and the shape of the beam bunch is approximated by a very short rectangular pulse.

Appendix B : Frequency Components of the Beam-Induced Field

The frequency components of the beam induced field have been measured by a spectrum analyzer. There have been observed four peaks as seer in Fig. B (1). The highest peak represents the resonant frequency of the 2/3 π mode. The two peaks on both sides of the highest peak represent the $\pi/2$ mode and 5/6 π mode, respectively, and the smallest peak at the left-hand side corresponds to the $\pi/6$ mode. The each peak is accompanied with many sidebands which are due to the pulsive change of the beam induced field.

It has turned out that the fundamental mode is more intensive than any other mode at least by 30 dB. The frequency components of the higher-order modes were not found in this measurement.

Appendix C : Change of the Stored Energy

The input admittance, Y_{in}, looking from the detuned short circuit plane into a cavity with beam loading can be written as

$$\frac{Y_{in}}{Y_o} = jQ_{ext\cdot 1}\left(\frac{\omega}{\omega_a'} - \frac{\omega_a'}{\omega}\right) + Q_{ext\cdot 1}\left(\frac{1}{Q_o} + \frac{1}{Q_{ext\cdot 2}} + \frac{1}{Q_b}\right) \quad , \qquad (C.1)$$

where Y_o is the characteristic admittance of the wave guide and the output wave guide of the cavity is assumed to be terminated by the matched load.

We write the input admittance as $Y_{in} = G + jB$, then the power flow into the cavity, P_{in} is expressed in the form

$$\frac{P_{in}}{P_o} = \frac{4(G/Y_o)}{[1 + (G/Y_o)]^2 + (B/Y_o)^2} \qquad (C.2)$$

where P_o is the input power.

Substituting the real and imaginary part of eq. (C.1) into eq. (C.2), we have

$$\frac{P_{in}}{P_o} = \frac{\dfrac{4}{Q_{ext\cdot 1}\, Q_L'}}{\left(\dfrac{1}{Q_{ext\cdot 1}} + \dfrac{1}{Q_L}\right)^2 + \left(\dfrac{2\Delta\omega}{\omega_a'}\right)^2} \quad , \qquad (C.3)$$

where

$$\frac{1}{Q_L'} = \frac{1}{Q_L} + \frac{1}{Q_{ext\cdot 2}} + \frac{1}{Q_b} \quad .$$

From the conservation law of the energy in the cavity, the stored energy is given by

$$W = \frac{Q_L'}{\omega} P_{in} \quad . \tag{C.4}$$

Thus from eqs. (C.3) and (C.4), the following equation for the stored energy is obtained

$$W = \frac{4P_o}{\omega Q_{ext\cdot 1}} \frac{1}{(\frac{1}{Q_{ext\cdot 1}} + \frac{1}{Q_{ext\cdot 2}} + \frac{1}{Q_o} + \frac{1}{Q_b})^2 + (\frac{2\Delta\omega}{\omega_a})^2} \quad , \tag{C.5}$$

References

1) C. S. Taylor and Y. Dupuis: Minutes of the 1964 Conference on Proton Linear Accelerators (MURA-714, Wisconsin, 1964) 239.

2) J. E. Griffin, IEEE Trans. on Nucl. Sci., NS-22 (1975) 1910.

3) J. Tanaka, H. Baba, I. Sato, S. Inagaki, S. Anami, T. Kakuyama, T. Takenaka, Y. Terayama, H. Matsumoto: Proceedings of the 1976 Proton Linear Accelerator Conference, ed. S. O. Schriber (AECL-5677, Ontario, 1976).

4) M. J. Lee: Proceedings of the 1968 Proton Linear Accelerator Conference Part 1 (BNL, New York, 1968) 114.

5) J. E. Leiss, IEEE Trans. on Nucl. Sci., NS-12 (1965) 566.

6) T. Nishikawa: Minutes of the 1964 Conference on Proton Linear Accelerators, (MURA-714, Wisconsin, 1964) 214.

7) T. Nishikawa, BNL Accelerator Department Int. Rep. AADD-87 (1965).

8) M. J. Lee: Proceedings of the 1968 Proton Linear Accelerator Conference Part 1 (BNL, New York, 1968) 108.

9) S. Giordano: Minutes of the 1964 Conference on Proton Linear Accelerators (MURA-714, Wisconsin, 1964) 252.

10) Jacques Marcou, Albert Papiernik, Albert Septier and Louis Wartski: C. R. Acad. Sc., t. 266 (1968) 134.

11) J. S. Fraser, J. Mokeown, G. E. McMichael and W. T. Diamond: Proceeding of the 1976 Proton Linear Accelerator Conference, ed. S. O. Schriber (AECL-5677, Ontario, 1976) 166.

12) T. Katayama, S. Arai, K. Yoshida and J. Tanaka, INS-Report 240 (1975).

13) J. C. Slater, Reviews of Modern Physics, 18 (1946) 441.

14) J. C. Slater: Microwave Electronics (Dover Publications, Inc., New York, 1950).

Figure Caption

Fig. 1. Schematic diagram of the experimental set-up, and the microwave apparatus.

Fig. 2. Photograph of the accelerator structure installed in the vacuum chamber.

Fig. 3. The waveform of the beam-induced field. Time scale = 0.5 μsec, amplitude scale = 10 mV/div.

Fig. 4. The stored energy due to the induced field in the structure is shown as a function of the beam current.

Fig. 5. The waveforms observed a) without bunch; b), c) with bunch on the accelerating phase and the decelarating phase, respectively. Time scale = 1 μsec/div., amplitude scale = 10 mV/div.

Fig. 6. The variation of the stored energy, the phase shift and the resonant frequency shift due to the beam loading. The theoretical results are shown by dotted line, dashed line and solid line.

Fig. 7. The diagram showing the phase relation of the bunches, the driving field and beam-induced field.

Fig. 8. The calculated values of the total loaded Q, Q_T, as a function of the relative phase of the bunch to the driving field, ϕ_b, where the loaded Q without beam loading is 10400.

Fig. b(1) The frequency component of the beam-induced field observed by spectrum analyzer. Horizontal scale = 5 MHz/div., vertical scale = 10 dB/div.

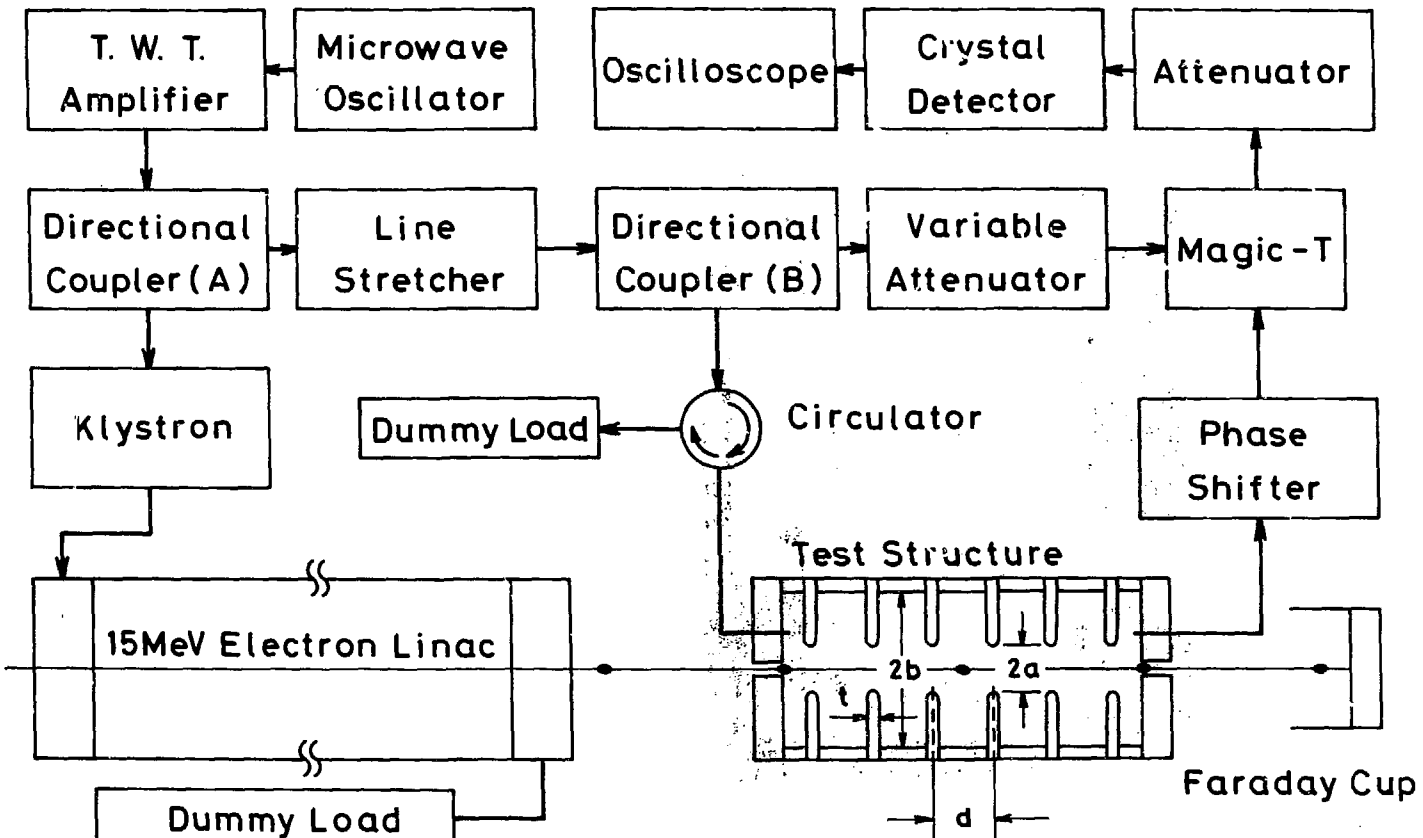
T. W. T. Amplifier
Microwave Oscillator
Oscilloscope
Crystal Detector
Attenuator
Directional Coupler (A)
Line Stretcher
Directional Coupler (B)
Variable Attenuator
Magic-T
Klystron
Dummy Load
Circulator
Phase Shifter
Test Structure
15MeV Electron Linac
2b
2a
t
Dummy Load
Faraday Cup
d

Fig. 1

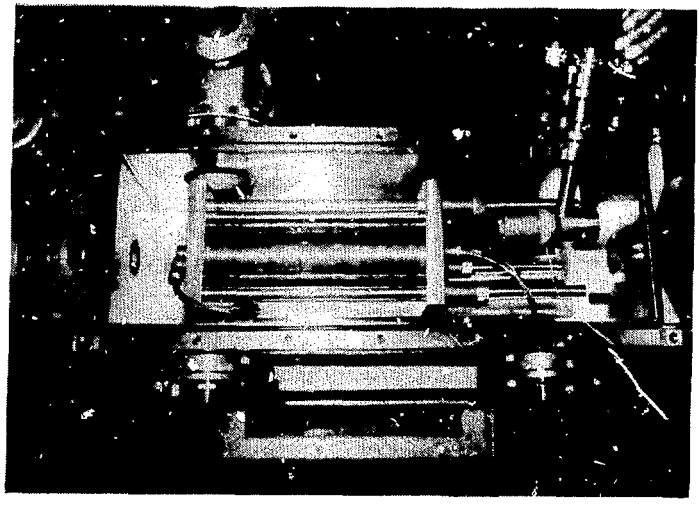

Fig. 2

Fig. 3

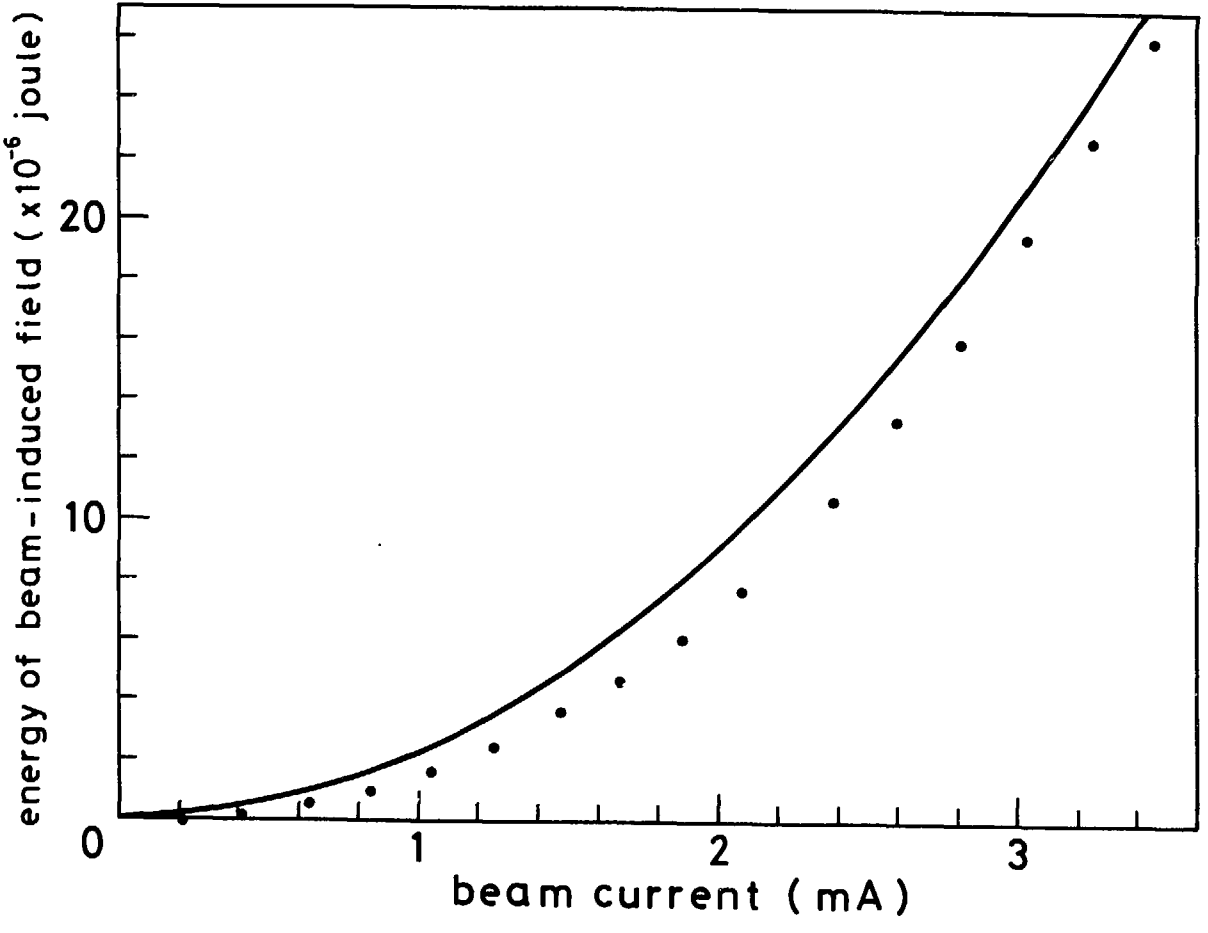
energy of beam-induced field (x10^{-6} joule)
20
10
0
1
2
3
beam current (mA)

Fig. 4

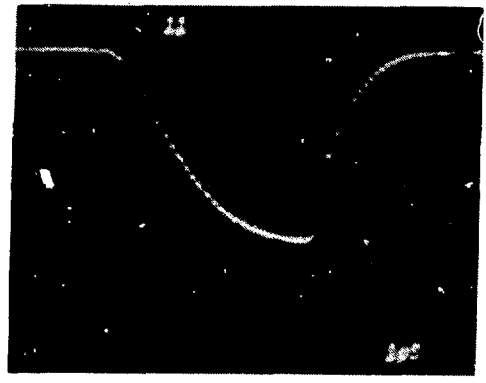

(a)

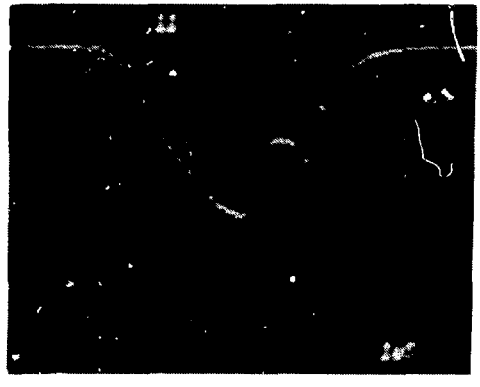

(b)

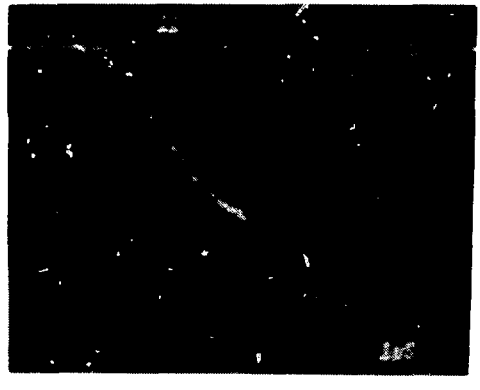

(c)

Fig. 5

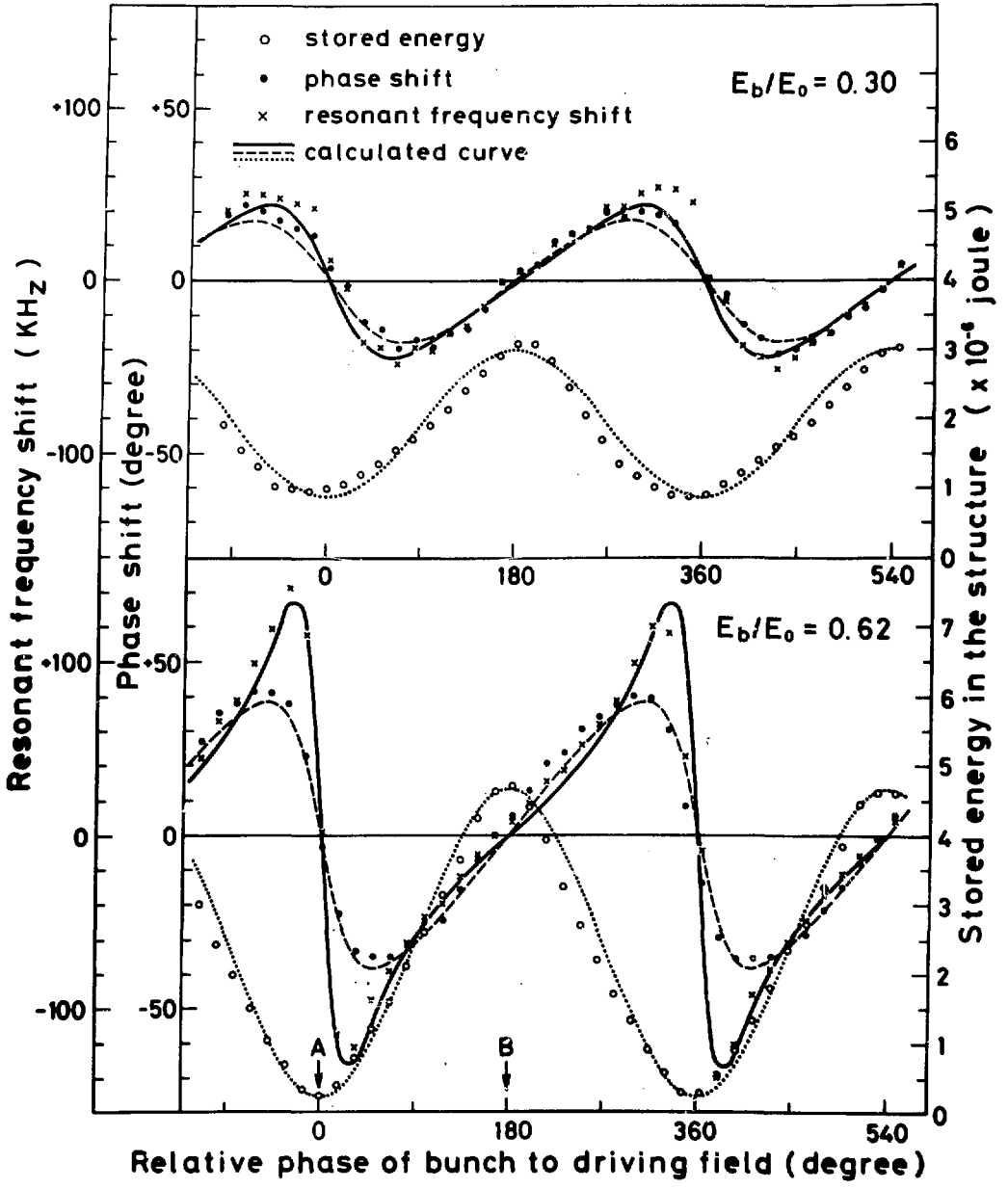
stored energy
phase shift
resonant frequency shift
calculated curve
$E_b/E_0 = 0.30$
$E_b/E_0 = 0.62$
Resonant frequency shift (KHz)
Phase shift (degree)
Stored energy in the structure (x 10^{-6} joule)
Relative phase of bunch to driving field (degree)
A
B
+100
+50
0
-100
-50
180
360
540
1
2
3
4
5
6
7

Fig. 6

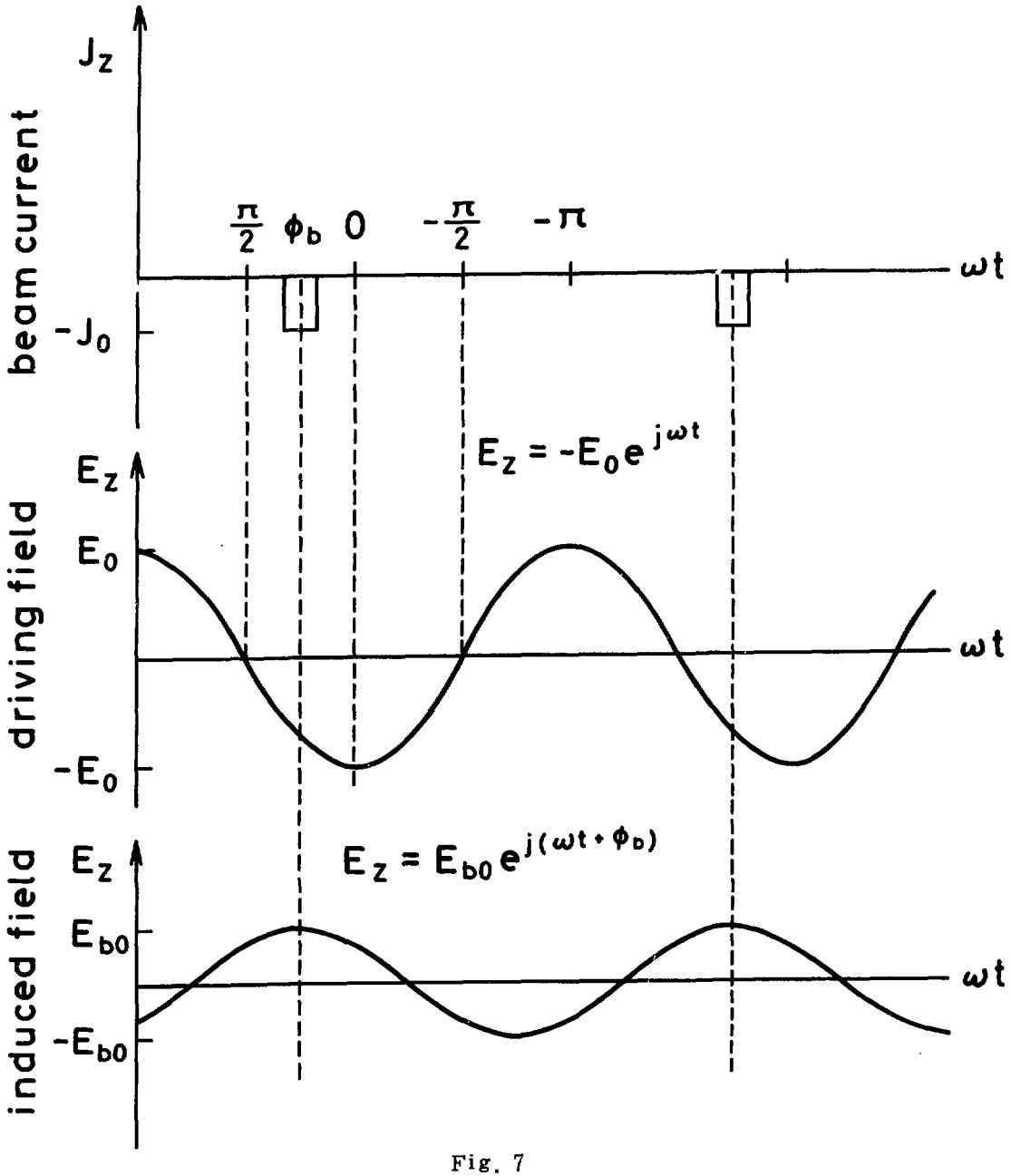
J_z
beam current
$\frac{\pi}{2}$ ϕ_b 0 $-\frac{\pi}{2}$ $-\pi$
ωt
$-J_0$
$E_z = -E_0 e^{j\omega t}$
E_z
driving field
E_0
ωt
$-E_0$
$E_z = E_{b0} e^{j(\omega t + \phi_b)}$
E_z
induced field
E_{b0}
ωt
$-E_{b0}$

Fig. 7

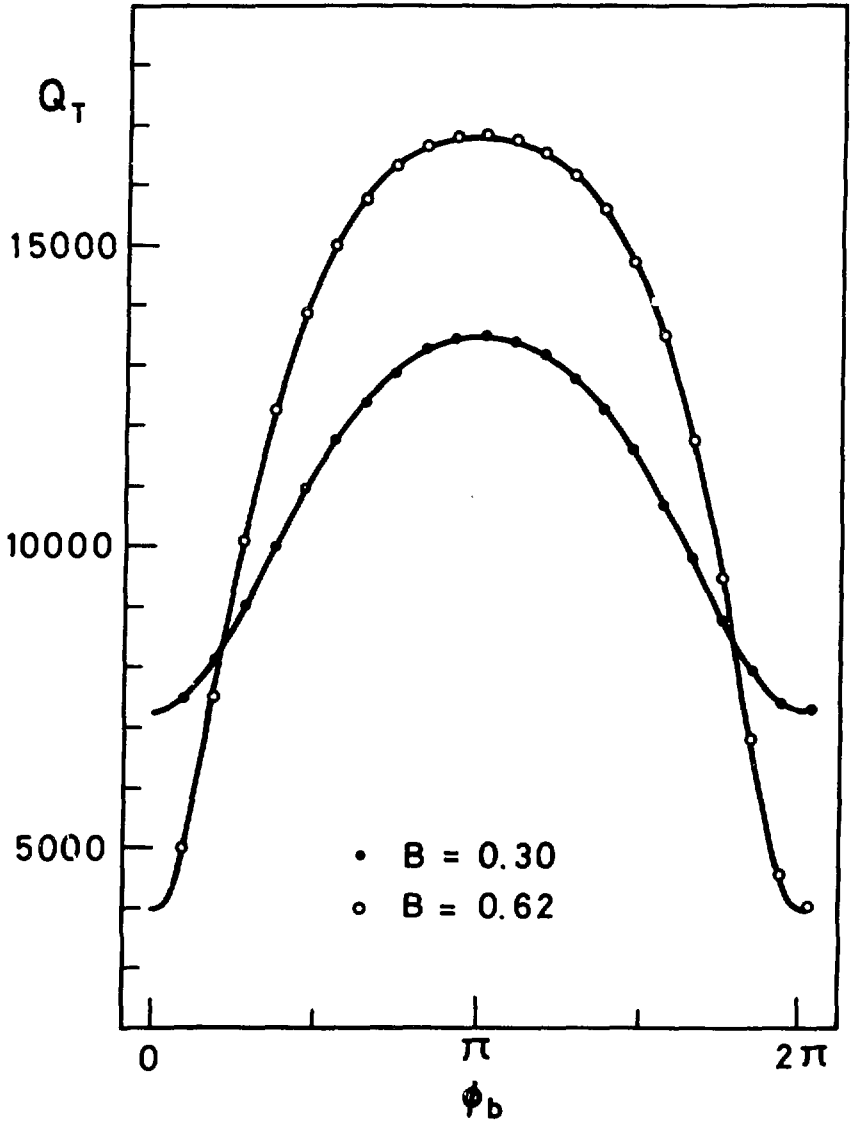

Fig. 8

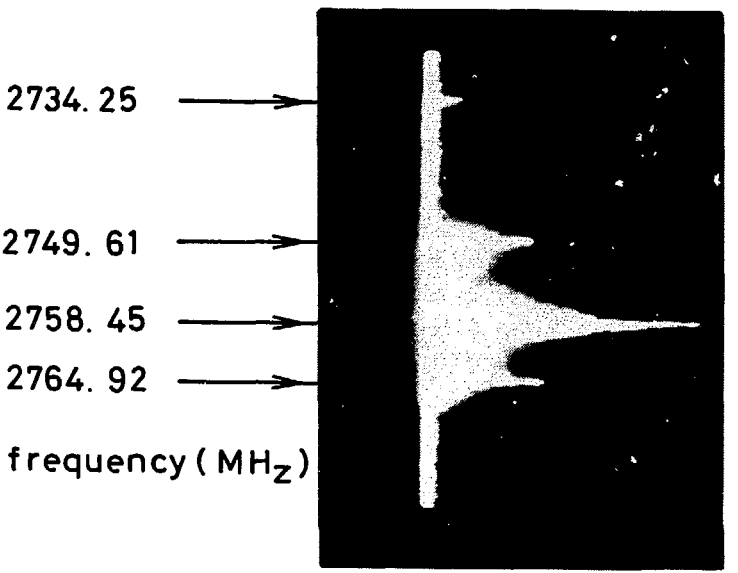

Fig. B(1)